Available online at www.sciencedirect.com

ScienceDirect

Physics Procedia 8 (2010) 33–38

Physics Procedia

www.elsevier.com/locate/procedia

VI Encuentro Franco-Español de Química y Física del Estado Sólido
VI[ème] Rencontre Franco-Espagnole sur la Chimie et la Physique de l'État Solide

Synthesis and characterization of $LiFePO_4$/C nanocomposites

Carmen Parada[1*], Carlos García Girón[1], Luis E. Fuentes[2] and Elena Gonzalo[3].

1. Dpto. Química Inorgánica. Fac. Ciencias Químicas UCM. 28040 (Madrid).
2. Centro de Investigaciones en Materiales Avanzados, 31109 Chihuahua (México).
3. Universidad San Pablo CEU. (Madrid).

Abstract

$LiFePO_4$/C nanocomposites have been synthesized by solid state reaction using iron oxalate, ammonium dihydrogen phosphate and lithium carbonate as $LiFePO_4$ precursors while carbon black was used as a carbon source. The mixtures were treated in a tubular oven under argon atmosphere at a temperature of 650 ºC and time intervals ranging between 2.5 and 1 hour for the three differently obtained samples. The effects of the time and temperature on their synthesis were investigated by X-ray diffraction (XRD), scanning electron microscopy (SEM) and magnetic measurements to determine the valence of iron. Carbon content in the composites was determined by means of EDX and Rietveld refinements.

Keywords: Li ion batteries, Cathode, $LiFePO_4$, Fast synthesis, X-ray diffraction, Morphology, Magnetic measurements.

1. Introduction

Since the original work of phospho-olivine, $LiFePO_4$ [1] has appeared to be a candidate for positive electrode materials for ion-lithium batteries, which is currently the subject of many investigations. It occurs in nature as the mineral triphylite, which crystallizes in an orthorrombic olivine structure in which lithium, iron and phosphorous occupy octahedral 4a, octahedral 4c, and tetrahedral 4c sites, respectively.

The Fe-O-P inductive effect generates a potential of ~3.5 V versus Li/Li^+ and a theoretical capacity of 170 mA h g^{-1} at moderate current densities [2]. $LiFePO_4$ exhibits several properties such as environmental friendliness, low price of the starting materials, high reversibility of the Li insertion/extraction, non toxicity and exceptional stability. When Li^+ ions and electrons are removed from $LiFePO_4$, the remaining $FePO_4$ has the same structure, with about 7% reduction in volume, which is advantageous for the achievement of a high cycle life.

* Corresponding author. Tel.: +34-13944355; fax: +34-13944352.
E-mail address: capa@quim.ucm.es

1875-3892
doi:10.1016/j.phpro.2010.10.008

Nevertheless, the main drawback of this material is its low intrinsic electric conductivity and poor lithium ion diffusion which result in losses of capacity during high-rate discharge. In order to solve these problems and to improve the rate performance of the olivine material, one possibility is to minimize the particle size [3], and also creates a large contact area with conductive additives such as carbon by forming composite materials [4]. Other strategies to improve its conductivity are being developed such as doping in Li-site to enhance intrinsic conductivity [5], co synthesizing the $LiFePO_4$/composites [6], etc.

Various syntheses methods such as sol-gel, coprecipitation, carbothermal reduction, etc, have been reported to optimize the particle size of $LiFePO_4$ [7-12]. In this work we present a new method to produce $LiFePO_4$ nanomaterials, reducing the energy consumption, cost and processing time required. In this way we have prepared nanocomposites $LiFePO_4$/C by a solid state reaction using two different strategies: a) Reducing the particle size by studying for the influence of temperatures and time treatments on the synthesis; b) Producing carbon composites.

2. Experimental

The syntheses of the $LiFePO_4$/C composites have been carried out by using the ceramic method in a tubular furnace under argon atmosphere. As raw materials Li_2CO_3, $Fe(C_2O_4)\cdot 2H_2O$ and $NH_4H_2PO_4$ (reagent grade) have been employed and carbon black was used as additive to form the composites. The use of carbon is not only to produce composites but also to avoid impurities of Fe(III) by creating a reductive atmosphere.

In order to achieve the reproducibility along the experiments we calculated the quantities of Li_2CO_3, $Fe(C_2O_4)\cdot 2H_2O$ and $NH_4H_2PO_4$ to get 0.5 g pure $LiFePO_4$ and after adding the carbon black in the proportions explained below. The weighted precursors were intimately mixed using an agate mortar and in each experiment the mixed powders were pressed at 75 MPa into pellets of 12 mm diameter each one.

Since one of the goals of this work was to yield nanoparticles, we have investigated the influence of the temperature on the syntheses processes, as most described experiments have used temperatures ranging between 750 ºC-900 ºC [13], but obtaining micron particles. We have also studied the influence of the heating time, given that in the previous works the heating time were not inferior to 10 h [14]. In this research we have considered the influence of the heating time making the syntheses for 2.5 h and for 1 h, respectively.

The thermal treatments for each material were: a) Sample I, obtained from precursors of $LiFePO_4$+carbon black in 100:10 ratio, heated to 650 ºC and then maintained for 2.5 h; b) Sample II, obtained from precursors of $LiFePO_4$+carbon black in 100:10 ratio, heated to 650 ºC and maintained for 1 h; c) Sample III, obtained only by precursors of $LiFePO_4$, heated to 650 ºC and maintained for 1 h. In all the cases after thermal treatments, the furnace was cooled naturally in the argon atmosphere to room temperature.

The X-ray diffraction patterns were recorded with a Philips X´Pert diffractometer with Cu Kα radiation (λ=1.540598 Å) operating at 45 KV and 40 mA. Data were measured over the range of 5-80º (2θ) with a step size of 0.02º and exposure of 5 s for routine characterization and over the range of 5-120º (2θ) with a step size of 0.0084 and exposure of 25 ms for structure refinements. These high resolution diffraction data obtained has been processed in a Rietveld refinement analysis with Fullproff programme [15].

The magnetic measurements have been measured with a super-conducting quantum interference device (SQUID) magnetometer. The magnetization M, was investigated in the range 4.2-300 K up to 1000 Oe.

Morphologies and sizes were observed by means of Scanning Electron Microscopy (SEM) carried out on a JEOL (Model JSM 6400); in addition, to confirm the oxidation state of the Fe, the magnetic measurements have been investigated because they are highly sensitive to a low impurity concentration of trivalent iron.

3. Results

The conditions of the syntheses are collected in Table 1 and X-ray diffraction patterns of I, II and III samples are shown in Fig.1. It can be observed that the diffraction profiles are similar in the three cases, corresponding to an

ordered olivine structure $LiFePO_4$, which crystallizes on to the orthorrombic system, S.G. Pnma. In composites I and II, it can be also assigned an additional reflection attributable to (2 0 0) of graphite, as it marked in the corresponding diffractograms.

Table 1: Syntheses conditions of the phases.

Sample	% $LiFePO_4$	% C_{black}	T_{max} (ºC)	t(h)
I	100	10	650	2.5
II	100	10	650	1
III	100	-	650	1

The Rietveld refinements allowed the determination of the lattice and structural parameters. The profile parameters of the pseudo-Voight function were used to describe the shape of the diffraction lines and the structural refinement was carried out by considering the $[Li]_{4a}[Fe]_{4c}PO_4$ structural hypothesis. In the Pnma space group of olivine structure, the Li, the (Fe, P, O_1, O_2) and O_3 ions occupy 4a (0,0,0), 4c (x,1/4,z) and 8d (x,y,z,) sites, respectively. The peaks profile was described with the Thompson-Cox-Hasting function for these composites. Isotropic models were shown to perfectly describe the size and strains effects, considering Lorentzian and Gaussian contribution, respectively. Only the parameters U and Y were refined, whereas V and W were fixed to the values obtained for LaB_6. From these refinements the cell parameters determined for the three samples are given in Table 2, in which it can be observed that the parameters are slightly smaller than those reported in the literature, probable due to its nanocrystalline character.

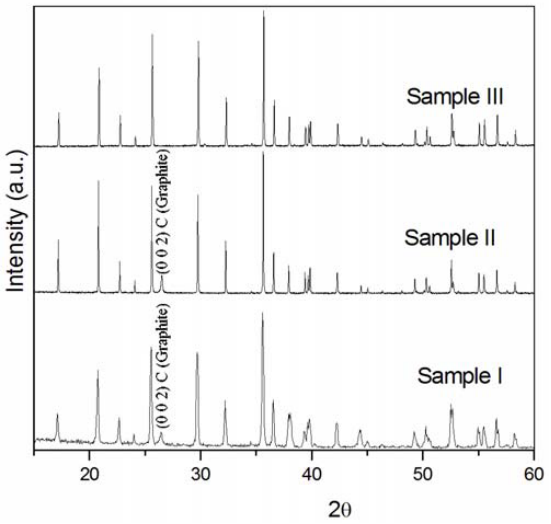

Figure 1. X-ray diffraction patterns of the samples I, II and III.

Fig.2, Fig.3 and Fig.4 gives a comparison of the experimental and calculated XRD patterns for the samples I, II and III, as well as the determined composition also from the Rietveld refinements that are showed on the respective insets. The rather small reliability factors (R_p, R_{wp} and R_{exp}) are shown in Table 3 in which, particles sizes of each component are also listed for the three materials determined by Rietveld refinements.

The quality of the agreement between observed and calculated profiles is measured by a set of nowadays conventional factors. In FullProf two sets of indices are calculated, according to the meaning of the integer N. In the first set N is the total number of points used in the refinement. In the second set only those points where there are

Bragg contributions are taken into account. The definition of the indices is as follows: The profile (Rp), the weighted profile (Rwp), the expected (Rexp) and the goodness of fit (χ^2). Less than 5 for Rp, Rwp and Rexp with a $\chi 2$ lower than 2 is considered a fine analysis, so we have made a very good analysis for samples I and III, and a good approximation with sample II. Therefore, the particle size of the sample III is slightly higher than the other samples, although sample I and sample II have been synthesized at the same temperature but shorter treatment time.

Table 2: Calculated lattice parameters of the samples.

Sample	$LiFePO_4$*	I	II	III
a(Å)	10.3713	10.327(5)	10.327(3)	10.329(5)
b(Å)	6.0216	6.006(2)	6.007(2)	6.007(1)
c(Å)	4.6625	4.691(3)	4.691(2)	4.691(4)

* From reference [6].

Table 3: Rietveld refinement results

Sample	R_p (%)	R_{wp} (%)	χ^2	R_{Exp}	$LiFePO_4$ (nm)	C (Graphite) (nm)
I	2.23	2.93	1.27	2.61	810.4	51.1
II	3.15	4.63	3.38	2.66	947.3	55.1
III	2.04	2.86	1.58	2.28	295.8	--------

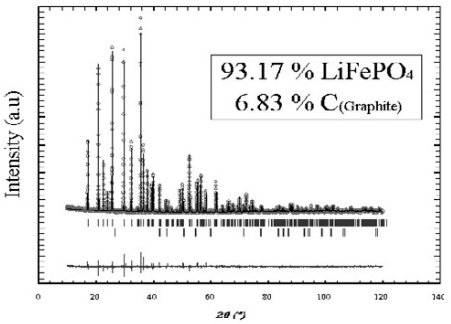

Figure 2. Experimental and calculated diffraction pattern of sample I.

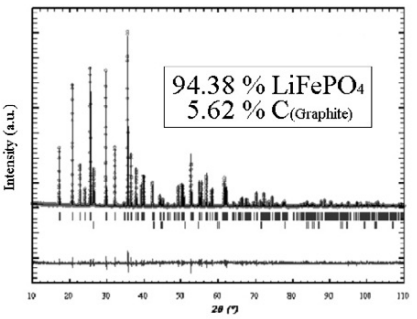

Figure 3. Experimental and calculated diffraction pattern of sample II.

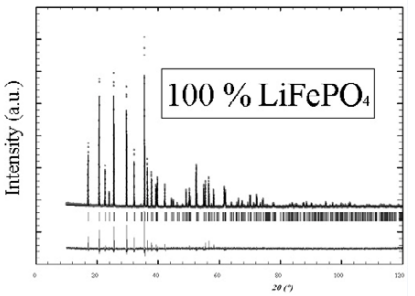

Fig.4 Experimental and calculated diffraction pattern of sample III.

The morphology of the samples have been investigated by means of Scanning Electron Microscopy, and in Fig.5 and Fig.6 it can be seen the size and morphology of the particles, corresponding to the micrographs of the samples I and II, respectively. As we can observe in Fig.5, the particle morphology consists of aggregates of primary nanoparticles about 400 nm, agglomerated in balls. Note that this spherical form was observed previously [15]. Fig.6 shows that these spherical particles develop on the surface of the graphite. This fact suggests not surprisingly that the carbon restrict the growing of the particles of the individual $LiFePO_4$. The composition of both type of particles, $LiFePO_4$ and graphite were determined by EDX on the scanning electron microscope. We also investigated the magnetic behaviour in composites in order to confirm the oxidation state of the iron. The magnetic properties of $LiFePO_4$ were reported in earlier publications [16]. The material undergoes a transition to antiferromagnetic order at

a Neel temperature T_N= 50ºC and therefore the magnetic investigations in these materials are useful to determine without ambiguity the oxidation state of Fe because some impurities of Fe(III) give another magnetic behaviour characteristic of ferromagnetic impurities [17]. As a representative example of the magnetic behaviour, Fig.7 shows the thermal evolution of the H/M ratio for sample III where H is the applied field fixed to 1000 Oe and M is the magnetization of the sample in which an antiferromagnetic transition can be observed at $T_N \approx 51$ K in good agreement with literature [18]. From the linear behaviour at $T \geq T_N$ we have calculated that the μ_{eff} per Fe ion is 5.32 MB, bigger than theoretical 4.98 MB predicted for Fe^{2+}. This fact observed previously [19] can be explained by the existence of Li vacancies on the structure, which is responsible for generating Fe^{3+} and consequently the disorder in the lattice. Therefore, this excess of effective magnetic moment in this material without impurities and without carbon additive can be attributed to a small concentration of Fe^{3+}.

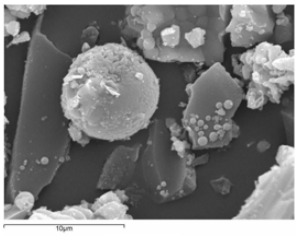

Figure 5. A SEM-micrograph of the composite I.

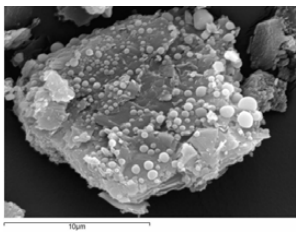

Figure 6. A SEM-micrograph of the composite II.

4. Conclusions

In order to cut down the cost and simplify the synthesis of $LiFePO_4$/C nanocomposites, they were synthesized from a mixture of iron oxalate, lithium carbonate, ammonium dihydrogen phosphate and carbon black as carbonaceous precursor, in a tubular furnace under argon atmosphere at a temperature of 650 ºC for2.5 and 1h. The three obtained materials were identified from a XRD point of view as pure olivine phases. The Rietveld refinements from XRD data have permitted to determine the compositions and the particle sizes of these three compounds. Nevertheless, the magnetic measurements indicated the existence of 5-6 % of Fe^{3+} on the structure, and the morphology observed by SEM showed the nanoparticles of $LiFePO_4$ in balls form.

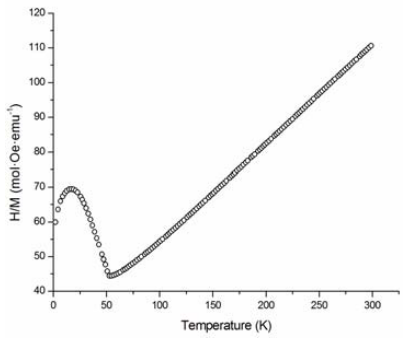

Fig.7 thermal evolution of the H/M ratio for sample III.

5. Acknowledgements

This research was financially supported by the MATYENER-505/PPQ/0358.CAM and Carlos García-Girón would like to thank Universidad Complutense de Madrid for financial support through the grant. S.E.M. micrographs and X-ray diffraction measurements were made on the "C.A.I. Luis Bru" and "C.A.I. DRX", respectively, that belongs to Universidad Complutense de Madrid.

6. References

[1] A.K. Padhi, K.S. Nanjundaswamy, J.B. Goodenough. J. Electrochem. Soc. 144(1997)1188.
[2] S. Franger, C. Bourbon, F. Le Cras. J. Electrochem. Soc. 151(2004)A1024-A1027.
[3] J. Barker, M.Y. Saidi, J.L. Swoyer. J. Electrochem. Soc. 6(2003)A53.
[4] P.S. Herle, B. Ellis, N. Coombs, L.F. Nazar. Nat. Mat. 3(2004)147.
[5] M.M. Doeff , J.D. Wilcox, R. Yu, A. Aumentado, M. Marcinek, R. Kostecki. J. Solid State Electrochem 12(2008)995.
[6] G. Rousse, J. Rodriguez-Carvajal, S. Patoux, C. Masquelier. Chem. Mater. 15(2003)4082.
[7] D. Wang, H. Li, Z. Wang, X. Wu, Y. Sun, X. Huang, L. Chen. J. Solid State Chem. 177(12)(2004)4582-4587.
[8] S.L., Bewlay, K. Konstantinov, G.X. Wang, S.X. Dou, H.K. Liu. Mater. Lett. 85(2004)1788.
[9] C.H. Mi, G.S. Cao, X.B. Zhao. Matter Lett. 59(2005)127.
[10] C.H. Chen, J.R. Dahn. J. Elecrochem. Soc. 149(2002)A1184.
[11] C.R. Sides, F. Croce, V.Y. Young, C.R. Martin, B. Scrosati. Electrochem. Solid-State Lett 8(2005)A484.
[12] J.F. Ni, H.H. Zhou, J.T. Chen, X.X. Zhang. Mater. Lett. 59(2005)2361.
[13] Z.G. Lu, M.F. Lo, C.Y. Cheng. J. Phys. Chem. C. 112(2008)7069.
[14] J. Rodríguez-Carvajal. Laboratoire Léon-Brillouin. http://www-llb.cea.fr/fullweb/powder.html (2004).
[15] J.M. Chen, Ch-H. Hsu, Y-R. Lin, M-H. Hsiao, G.T.K. Fey. J. Power Sources 184(2008)498.
[16] R.P. Santoro, R.E. Newnhann, S. Nomura. J. Phys. Chem. Solids 27(1966)655.
[17] N. Ravet, M. Gautier, K. Zaghib, J.B. Goodenoug, A. Mauger, F. Cendron, C.M. Julien. Chem. Mat. 19(10)(2007)2595.
[18] M. Maccario, L. Croguennec, A. Wattiaux, E. Suard, F. Le Cras, C. Delmas. Solid State Ionics 179(35-36)(2008)2020-2026.
[19] A. Mauger, K. Zaghib, F. Gendron, C. Julien. Ionics 14(2008)209.